Accepted Manuscript

Title: Feasibility study and performance evaluation of low capacity water-LiBr absorption cooling systems functioning in different algerian climate zones

Author: Omar Ketfi, Mustapha Merzouk, Nachida Kasbadji Merzouk, Mahmoud Bourouis

PII: S0140-7007(17)30281-5
DOI: http://dx.doi.org/doi: 10.1016/j.ijrefrig.2017.07.002
Reference: JIJR 3702

To appear in: *International Journal of Refrigeration*

Received date: 18-4-2017
Revised date: 19-6-2017
Accepted date: 2-7-2017

Feasibility study and performance evaluation of low capacity water-LiBr absorption cooling systems functioning in different Algerian climate zones

Omar Ketfi [a, c], Mustapha Merzouk [b], Nachida Kasbadji Merzouk [c], Mahmoud Bourouis [d *]

[a] Mechanical Department, Faculty of Technology, University of Blida 1, Blida, Algeria.
[b] Renewable Energy Department, Faculty of Technology, University of Blida 1, Blida, Algeria.
[c] Unité de Développement des Equipements Solaires/UDES/CDER, 42415, W. Tipaza, Algeria.
[d] Department of Mechanical Engineering, Universitat Rovira i Virgili,
Av. Països Catalans No. 26, 43007 Tarragona, Spain.

[*] Corresponding author.
Email: mahmoud.bourouis@urv.cat

Highlights

1. Water-LiBr absorption chillers were analysed in the five climate zones in Algeria.
2. In zones E1 and E2, the chillers produced chilled water at 7 ºC and partial charge.
3. In the hot zones E3, E4 and E5, it was not feasible to produce chilled water at 7ºC.
4. The chillers were able to produce chilled water at 12ºC in zones E3 and E4.
5. The chillers were not able to operate under the thermal conditions of zone E5.

Abstract

A performance analysis was carried out on water-LiBr absorption chillers performing in the five different climate zones in Algeria. A 17.6 kW single-effect and a 16 kW double-effect commercial absorption chillers were simulated. In climate zones E1 and E2, the single-effect and double-effect chillers supplied 37% and 91% respectively of their nominal capacity to produce chilled water at 7°C. In the hot climate zones E3, E4 and E5, it was not feasible for either of the chillers to produce chilled water at 7ºC. By increasing the chilled water temperature to 12°C both absorption chillers were able to operate in climate zones E3 and E4. The single-effect chiller reached 45% of its nominal capacity in zone E3 and 33% in zone E4. The double-effect chiller delivered 80% of its nominal capacity in both climate zones. Neither of the chillers was able to operate under the thermal conditions of climate zone E5.

Keywords: Thermal cooling; absorption chillers; water-LiBr; climate zones in Algeria

Nomenclature

x	Mass concentration of LiBr	
m	Mass flow rate	[kg s^{-1}]
Q	Heat duty	[kW]
h	Enthalpy	[J kg^{-1} K^{-1}]

Abbreviations

LiBr	Lithium Bromide
H_2O	Water
HEX	Heat exchanger
HP	High pressure
LP	Low pressure

Subscripts

i	Inlet
o	Outlet

1. Introduction

The air conditioning sector is one of the major consumers of energy in Algeria because of the hot summers experienced in most areas of the country. Taking into account the great potential of solar energy available in the country (169400 Twh/year; CDER (2010)), thermally driven air-conditioning systems are a very attractive way of reducing the amount of electricity consumed by conventional vapour compression systems.

Several studies focused on solar cooling systems are available in the open literature. Al-Alili et al. (2014) presented an overview on solar thermal cooling technologies, i.e. absorption, adsorption and ejector cooling systems. The authors reported that solar absorption cooling systems showed an average collector area of 4.67 m^2 kW^{-1}, a normalized thermal storage of 0.21 m^3 kW^{-1} and a coefficient of performance of 0.68 at an average heat source temperature of 88.5 ºC. Siddiqui and Said (2015) reviewed the research published on solar powered absorption cooling systems, diffusion-absorption systems, ejector based absorption systems, compression absorption systems and cogeneration/trigeneration absorption systems. Their review included the thermodynamic properties of new working pairs proposed for solar cooling technologies. Along with the wide use of water-LiBr and ammonia-water fluid mixtures, other working pairs, such as ammonia-lithium nitrate, ammonia-sodium thiocyanate and water-LiCl, also performed well.

Hidalgo et al. (2008) experimentally investigated a solar powered water-LiBr absorption chiller at the University Carlos III of Madrid, Spain. The chiller was powered by 50 m^2 of vacuum tube solar collectors. The chiller was used as an air-conditioner in a detached house with a 90 m^2 floor space. A peak cooling capacity of 6 to 8 kW was recorded for 6.5 h with a total solar fraction of 56%, and a seasonal cooling energy of 23 kWh/day was supplied by the system. Mammol et al. (2010) carried out an experimental study on a solar heating and cooling system in New Mexico. The system was composed of a 70 kW Yazaki water-LiBr absorption machine powered by 124 m^2 of flat-plate solar collectors and 108 m^2 of evacuated solar collectors. Four different control strategies were implemented for: summer daytime, summer night time, winter daytime and winter night time. Seven cold storage tanks of 50 m^3 each and a 34 m^3 hot water storage tank were used. The authors reported that the solar cooling system was able to supply approximately 18% of the total cooling demand at the peak of summer, and that this rate could be increased to 36%. Moreover, 100% of the cooling and heating demands were supplied by the solar powered system in winter and in fall seasons. Bermejo et al. (2010) presented an experimental study of a 174 kW double-effect absorption chiller powered by natural gas and 352 m² of linear concentrating Fresnel collectors in Seville, Spain. The solar cooling system delivered an average daily cooling capacity of 135 kW (77% of the nominal capacity) with a coefficient of performance ranging from 1.1 to 1.25 when the heat source temperature was set at 145 ºC. The solar heat and solar cooling fractions were 0.75 and 0.44, respectively. Bujedo et al. (2011) tested three control strategies in an absorption solar cooling plant installed in Boecillo, Spain. The first strategy was based on full load operation with On-Off control, the second strategy consisted in adapting the condenser temperatures to those of the generator and regulating the load by On-Off cycles, and the last strategy was similar to the second one, but regulated the load by means of the heat source flow. The cooling system consisted of a 35 kW Yazaki water-LiBr absorption chiller, 40 m² of evacuated solar collectors and 37.5 m² of flat plate solar collectors with two 2 m^3 storage tanks. The authors reported that the third control strategy was the best of the three with an increase of 12.6% in solar field efficiency and 48.17% in total efficiency when compared with the first control strategy. Rosiek and Batlles (2012) experimentally investigated a 70 kW Yazaki water-LiBr single-effect absorption chiller installed in the Solar Energy Research Center (CIESOL) in Almeria, Spain. Two cooling systems were used to dissipate the heat released in the absorber and condenser, namely a 170 kW cooling tower and a shallow geothermal cooling system. The absorption chiller was powered by 160 m² of flat-plate solar collectors. Using the cooling tower system, the chiller delivered between 68% and 70% of its nominal cooling capacity when the generator, absorber/condenser and evaporator return temperatures were set at 75.8, 27.6 and 15.2 °C, respectively. Using the shallow cooling system, a cooling capacity rate of up to 74% was achieved with generator, absorber/condenser and evaporator return temperatures of 71, 26.8 and 14.3 °C, respectively. These results were quite similar in both cases; however, in the case of the shallow cooling system, significant savings were obtained in terms of a reduction in CO_2 emissions and in the consumption of electric power and water. Albers (2014) developed a new control strategy for an air-conditioning installation in the Federal Environment Agency in Dessau, Germany. This strategy was based on controlling the hot and cooling water inlet temperatures simultaneously in order to increase solar fraction and/or to decrease system costs. The solar cooling system integrated a 23.3 kW absorption chiller which replaced an adsorption chiller of the same cooling capacity. The driving thermal energy was supplied by, either a combined heat and power plant, or by 216 m² of vacuum solar collectors with three 7.5 m^3 hot storage tanks. The absorption system showed an increase of 62% and 35% in thermal and electrical efficiency, respectively, and saved 68% in water consumption compared to the previous adsorption chiller.

Other investigations discussed the feasibility of absorption air-conditioning systems in different climatic conditions. Sarabia et al. (2011) investigated a small size water-LiBr absorption chiller powered directly by 8 m² of solar vacuum collectors without heat storage working in five climate zones in Spain. The authors reported that there was a significant decrease of up to 60% in the cooling capacity when there was insufficient solar power to drive the absorption chiller. This sharp decrease in cooling capacity could be solved by increasing the surface area of solar collectors. Darkwa et al. (2012) reported on the performance analysis of a 55 kW water-LiBr absorption chiller powered by 220 m² of evacuated tubular solar collectors and a storage volume of 16 m^3 working in a sub-tropical environment in China. The results were presented for a typical day in August 2011 and the coefficient of performance was 0.69 at generator temperatures ranging from 91 to 96 ºC. For an ambient temperature of 36 °C, the chiller delivered 82% of its nominal cooling capacity. Li et al. (2016) presented an experimental study of a 23 kW water-LiBr absorption cooling system working in the climatic conditions of Kunming, China. The system was powered by 56 m² of parabolic through collectors and built to ensure an air-conditioning supply to a 102 m² meeting room. For a typical sunny day, the coefficient of performance of the chiller ranged from 0.18 to 0.6 with a solar fraction between 0.33 and 0.41. Viñas et al. (2016) studied the performance of a 35 kW Yazaki water-LiBr absorption chiller driven by liquefied petroleum gas (LPG) and 220 m² of evacuated solar collectors working in two areas on the coast of Mexico, namely Campeche and Acapulco. The maximum ambient air temperature registered, respectively, for these two cities was 39.4 ºC and 33.7 ºC. This solar cooling system supplying air-conditioning to eight residential houses was investigated. The temperature in the houses was kept at warm and comfortable thermal conditions (24 to 28°C), the maximum monthly heat extraction was 3.21 10^6 kJ and 3.36 10^6 kJ in climatic conditions in Campeche and Acapulco, respectively. Agrouaz et al. (2017) presented a theoretical study of a 10 kW solar absorption air-conditioning system working in six different climate regions in Morocco. In the city of Errachidia the system performed best during the months registering peak-loads. The solar fraction was 45% and COP was 0.3.

This paper presents a performance analysis of small capacity water-LiBr absorption chillers functioning in five different climate zones in Algeria. These climate zones are specific to the CNERIB classification (1993), where the first two zones (E1, E2) are the littoral and the highlands, respectively, while the other three (E3, E4 and E5) represent the pre-Sahara and the heart of the Algerian Sahara. These three zones are characterised by a hot and arid climate. Two commercial absorption chillers were selected as case studies; a 17.6 kW Yazaki single-effect absorption chiller and a 16 kW Broad double-effect absorption chiller. The coefficient of performance and the cooling capacity of the chillers were analysed for each climate zone. Previously, a parametric study had been carried out varying the thermal conditions of the cooling medium and heat source.

2. ALGERIAN CLIMATE ZONES

The Algerian climate is known by its diversity, the northern climate (coastal zone) is similar to that of other Mediterranean countries. Further south, the climate begins to change with colder winters and hotter summers. Different studies were carried out to define and locate the different climate zones in Algeria; two of them are herein summarized. The first classification was presented by J. Borel (1962) who proposed 7 climate areas including one sub-area for winter and summer periods. The second classification, in which five climate zones were proposed for summer periods, was reported in 1993 by the National Centre for Studies and Research Integrated Building (CNERIB) of Algeria, Belgaid (2011). This classification, shown in Figure 1, was selected for the present work as it best describes the Algerian climate.

Table.1 shows a summary of the climatic data for the five climate areas in Algeria, these data were provided by the National Meteorological Office (ONM), Belgaid (2011). The average minimum and maximum temperatures as well as the average solar irradiation for the hottest month of the year (July) were presented using the CNERIB classification. In this table, it is seen that the costal and highland zones (E1 and E2) are characterised by an average maximum temperature of 30.6 and 34.5 °C, respectively, while the three last climate zones (E3, E4 and E5) are characterised by a maximum ambient air temperature ranging from 40 to 45 ºC. The important solar irradiation potential is particularly noteworthy especially that of the latter three zones, and this makes the use of solar thermal energy very suitable for driving air-conditioning systems in these areas.

3. MODELLING OF ABSORPTION CHILLERS

The single-effect and double-effect water-LiBr absorption cooling cycles were modelled and simulated using the Matlab simulation tool. Two commercial absorption chillers were considered in this work: a 17.6 kW single-effect chiller manufactured by Yazaki Corporation and a 16 kW double-effect parallel-flow chiller manufactured by Broad Corporation. The cycle configurations of both absorption chillers, represented in Figures 2 and 3, were taken from the manufacturers' catalogues. In the case of the parallel flow double-effect cycle, the solution flow-rate leaving the absorber is split into two parts, 40% is pumped to the low pressure generator and 60% to the high pressure generator (Balghouthi et al. (2012)).

The mathematical model was based on the partial and overall mass balances and energy balance in each component of the absorption cycles and the equilibrium considerations and thermodynamic properties of the working fluids. A Matlab simulation programme, which included the thermodynamic properties of water-LiBr, was developed to simulate each one of the configurations analysed.

The main equations of the mathematical model are as follows:

- Total mass conservation

$$\sum m_i = \sum m_o \qquad (1)$$

Where m_i and m_o are respectively the inlet and outlet mass flow rates [kg s^{-1}]

The absorbent conservation is expressed by:

$$\Sigma(m_i\ x_i) = \Sigma(m_o\ x_o) \qquad (2)$$

Where x is the LiBr solution concentration.

- The energy balance in each thermal component of the absorption cycle is expressed by the general equation **:**

$$\Sigma((m_i\ h_i) - (m_o\ h_o)) + Q = 0 \qquad (3)$$

Where Q is the heat exchanged in the component.

The assumptions and equilibrium considerations taken into account are summarized as follows:

- Steady-state operation mode.
- Streams leaving the main components (absorber, generator, condenser and evaporator) are at saturation state.

- Pressure drops are negligible except in the throttling devices.
- Pumping work is negligible.
- Heat losses or gains from the surroundings are negligible.
- Pumping and throttling processes are isenthalpic.

The thermodynamic properties of the water-LiBr fluid mixture were taken from the model developed by Patek (2006). Moreover, a crystallization test was implemented in the simulation programme setting a safety temperature margin of 5°C; the solution entering the absorber is more likely to be exposed to crystallization due to the low temperature and high concentration in salt. The crystallization temperature of the solution was estimated by the expression of Eq. (4) and depending on the solution concentration X (Tesha (2009)):

$$T_{crit} = A\,X^2 + B\,X + C \tag{4}$$

A, B and C are given in Table 2.

The efficiency parameters used to analyse the performance of the absorption cycles under the climatic conditions of the different zones were those of the coefficient of performance (COP), which is the ratio of the evaporator thermal load by the driving heat supplied to the generator, and the cooling capacity.

After introducing the temperatures of the chilled water and heat source, the simulation programme required that the climate zone under study be specified, or that the climatic data of the simulation be introduced manually. The simulation was then started and followed the sequence described below:

- The pressure levels were calculated based on the properties of pure water and using REFPROP database and IAPWS formulations (IAPWS (1995)).
- The salt concentrations in the solution circuits were determined using the correlations reported in ASHRAE (2009).
- After calculating the mass flow rates, the enthalpy of the different streams in the cycles was calculated (Patek (2006)).

- The crystallization test was then performed and the chiller efficiency parameters calculated.

4. RESULTS AND DISCUSSION

The operation and performance of the Yazaki single-effect and Broad double-effect absorption chillers were analysed in the thermal conditions in the five climate zones in Algeria. Previously, the model developed was validated using the experimental data obtained by Rodrigez (2013) on the Yazaki absorption chiller and a parametric study varying the temperatures of the three external circuits i.e. cooling medium, heat source and chilled water was carried out for both absorption chillers. The nominal conditions of the two commercial absorption chillers and intervals of the input parameters used in the parametric study are summarized in Table 3. Neither the solution mass flow rates, nor the heat exchanger efficiencies, were given by the manufacturers of the two commercial chillers so they were taken from the experimental studies reported by Martinez et al. (2016) for the Yazaki chiller and Balghouthi et al. (2012) for the Broad chiller. The temperature gradient (ΔT) of each component was selected in terms of the heat exchange nature, namely 3°C for the evaporator and generator (liquid-liquid heat exchange) and 7.5 °C for the condenser and absorber taking into account that there was an indirect air cooling mode.

4.1 Model validation

The simulation results obtained with the cycle configuration of the Yazaki absorption chiller were then compared with the experimental data reported by Rodriguez (2013) for the same chiller. The thermal loads of the generator and evaporator and the heat rejected by the absorber and condenser are shown in Figure 4 at different temperatures of the heat source. As can be observed, the simulation results are well in agreement with experimental data, with the deviations around 10, 8 and 1% for the generator and evaporator thermal loads and rejected heat, respectively.

4.2 Parametric study

A parametric study was carried out to analyse the effect of the temperature of the heat dissipation medium, driving heat and chilled water on the performance of both commercial absorption chillers considered in the present work. The ambient air temperature was varied from 26 to 46 ºC at 2 ºC intervals and the heat source temperature from 80 to 110 ºC for the single-effect absorption chiller and from 118 to 160 °C for the double-effect absorption chiller also at 2 °C intervals. Two temperatures were applied for the chilled water, namely 7 ºC and 12 ºC. In order for the single-effect configuration to achieve a COP higher than 0.6 and for the double-effect configuration a COP higher than 1.0, feasible intervals of ambient air temperature were established.

The 3D figures 5 and 6 show, respectively, the variations of the coefficient of performance (COP) and cooling capacity versus the ambient air and heat source temperatures at 7 ºC and 12 ºC of chilled water temperatures for the Yazaki single-effect absorption chiller. The 3D figures 7 and 8 illustrate the same trends for the Broad double-effect absorption chiller. It is noteworthy that the functioning area of the absorption chillers is represented by the coloured zones, while the non-functioning areas are represented by the dead zones on the right side (temperature of the driving heat is insufficient) and on the left side (crystallization of the working fluid water-LiBr).

Figures 5 and 6 show that the single-effect absorption chiller reached a COP higher than 0.6 when it was operated at an ambient air temperature ranging from 30 ºC to 40 ºC for the production of chilled water at a temperature of 7 ºC and from 30 to 44 ºC for chilled water at a temperature of 12 ºC. As observed in these figures, the cooling capacity with a COP higher than 0.6 varied from 11.7 to 4.3 kW for chilled water at 7 ºC and from 16 to 3 kW for chilled water at 12 ºC. With regard to the quantitative effect of ambient air temperature on the chiller performance, it was seen that when the ambient air temperature was increased from 30 ºC to 40 ºC and chilled water temperature was set at 7 ºC the coefficient of performance and cooling capacity decreased by 15% and 63%, respectively. The corresponding degradation rates were 9% and 48% when the chilled water temperature was set at 12ºC.

Regarding the double-effect absorption chiller, figures 7 and 8 show that COP values were above 1.0 when the chiller was operated at an ambient air temperature ranging from 30 ºC to

40 ºC and chilled water temperature was set at 7 ºC. The corresponding range of ambient air temperature was 30º-44 ºC when the chilled water was set at 12ºC. The cooling capacity delivered by the chiller with a COP higher than 1.0 varied from 23 to 10 kW for the ambient air temperature range with chilled water set at 7 ºC and from 31 to 8 kW for the ambient air temperature range with chilled water set at 12 ºC. Moreover, by increasing the ambient air temperature from 30 ºC to 40 ºC, the coefficient of performance and cooling capacity of the chiller were reduced by 11% and 56%, respectively, with chilled water set at 7 ºC and by 8% and 44%, respectively, with chilled water set at 12 ºC.

4.3 Performance analysis of single-effect and double-effect water-LiBr absorption chillers functioning in different Algerian climate zones

The operational feasibility and performance of the two small capacity commercial water-LiBr absorption chillers considered in the present work are herein presented for each one of the five Algerian climate zones. Two values were contemplated for chilled water temperature, namely 7 ºC and 12 ºC. The condensation temperature was implicitly obtained from the maximum ambient air temperature of each climate zone. Figures 9 to 12 show the efficiency parameters obtained for both Yazaki single-effect and Broad double-effect absorption chillers working in the five climate zones.

Figures 9 and 10 show the variation of the coefficient of performance (COP) and cooling capacity, respectively, versus the heat source temperature for the single-effect absorption chiller at chilled water temperatures of 7 and 12 ºC. It is worthy of note that the absorption chiller was able to produce chilled water at 7 ºC in climate zones E1 and E2 with a COP of 0.72 and 0.70 and with heat source temperatures of 90 °C and 100 °C, respectively (Fig. 9a). However, this chiller was not able to produce chilled water at 7 ºC at the high ambient air temperatures (40 to 45 ºC) of climate zones E3, E4 and E5. This was due to crystallization problems or very low efficiency. To overcome this limitation, the chilled water temperature was increased to 12 ºC so that the absorption chiller could operate in the climatic conditions of zones E3 and E4. Consequently COPs of 0.71 and 0.68 were, respectively, obtained at a heat source temperature of 110 ºC (Fig. 9b).

A cooling capacity of 6.5 kW was obtained for climate zones E1 and E2 at heat source temperatures of 90 and 100 ºC, respectively, and a chilled water temperature of 7 ºC (Fig.

10a). This represents around 37% of the nominal cooling capacity and was due to the indirect cooling of the absorber and condenser considered in the present work. Depending on the ambient air temperature, this cooling mode significantly increased the absorber and condenser temperatures. At 110 ºC of the heat source temperature, the cooling capacities were 16.35 and 11.45 kW for climate zones E1 and E2, respectively, i.e. 93% and 65% of the nominal value. By increasing the chilled water temperature to 12 ºC (Fig. 10b), the cooling capacity of the chiller operating in climate zones E1 and E2 was increased by 5% and 12%, respectively. Moreover, at a heat source temperature of 110 ºC, cooling capacities of 7.9 kW for zone E3 and 5.8 kW for zone E4 were obtained, i.e. 45% and 33% of the nominal cooling capacity.

It is important to mention that the single-effect absorption chiller was not able to produce chilled water at 7 ºC or 12 ºC in the climatic conditions of zone E5. This was due to the high ambient air temperature of the zone and the indirect heat dissipation taken into account in the present work, both of which lead to a temperature increase in the absorber and condenser.

The variations of the coefficient of performance (COP) and the cooling capacity, versus the heat source temperature, are shown in figures 11 and 12 respectively, for the double-effect absorption chiller at chilled water temperatures of 7 and 12 ºC. At a chilled water temperature of 7 ºC, the COPs of the chiller were 1.20 and 1.17 for climate zones E1 and E2 with heat source temperatures of 140 ºC and 150 ºC, respectively (Fig. 11a). It is important to note that, in this case, the chiller was also able to operate in zones E3 and E4 with a COP higher than 1.0 and with a heat source temperature of over 160 ºC. When a chilled water temperature of 12 ºC was applied, the heat source temperature required to drive the absorption chiller was about 10 ºC lower than that of the chilled water at 7 ºC and the COP also improved (Fig. 11b). The COP values were 1.15 and 1.14 at heat source temperatures of 155 ºC and 160 ºC for climate zones E3 and E4, respectively. Regarding climate zone E5, the chiller was not able to operate at 7 ºC or 12 ºC of chilled water temperature regardless of whether the heat source applied was at a high temperature.

The cooling capacities obtained for climate zones E1 and E2 reached about 14.6 kW when heat source temperatures of 140 and 150 ºC, respectively were applied, and the temperature of the chilled water was set at 7 ºC (Fig. 12a). This cooling capacity represented around 91% of the nominal cooling capacity. This was due to the indirect cooling of the absorber and condenser considered in the present work. Nominal cooling capacity was achieved at a heat source temperature of 142 ºC for climate zone E1 and 152 ºC for zone E2. The cooling capacity delivered by the chiller in the climatic conditions in zones E3 and E4 was much lower than the nominal value (16 kW) even at high heat source temperatures. With the heat source at 160 ºC, the cooling capacities of the chiller were 9.5 kW for zone E3 and 6 kW for zone E4. By increasing the chilled water temperature to 12 ºC, the cooling capacity of the chiller operating in climate zones E1 and E2 was increased by 38% and 32%, respectively (Fig. 12b). Moreover, a cooling capacity of 13 kW was obtained in climate zones E3 and E4 at heat source temperatures of 155 °C and 160 °C, respectively, i.e. 80 % of the nominal cooling capacity. Notably, the cooling capacities delivered by the double-effect absorption chiller were significantly higher than those obtained by the single-effect absorption chiller operating in the same climatic conditions of these zones (E3 and E4).

Regarding climate zone E5, the results showed that neither the single-effect nor the double-effect water-LiBr absorption chiller was feasible for use there, either due to the crystallization of the water-LiBr solution or because efficiency was very poor. The absorber and condenser had to operate at high temperatures which increased the salt concentration of the strong solution in the absorption cycle and consequently increased the risk of crystallization of the solution. Water-LiBr solution has a limited range of solubility which restricts the range of temperatures feasible for the absorber. To overcome this limitation, the following options could be considered.

- A geothermal heat exchanger could be used to dissipate the heat released in the absorber and condenser. It is well known that in summer, the soil temperature is lower than that of the ambient air and this temperature remains almost constant throughout the year at a given depth below ground level. Therefore, in places with hot arid climates this layer below the ground could be used as a heat sink for the absorption chiller.
- Recent investigations have shown that addition of other salts to LiBr aqueous solutions can significantly improve the solubility of the solution. However, the criteria for selecting an appropriate salt mixture should not only consider an increase in the solubility range, but also other aspects of machine operation such as vapour pressure, viscosity, corrosion, thermal and chemical stability. Bourouis et al. (2005) and Asfand et al. (2016) reported that the aqueous solution of the quaternary salt system ($LiBr+LiI+LiNO_3+LiCl$) is recommended for absorption chillers operating at high absorber and condenser temperatures. They also reported that the working pair water-

LiBr+LiI+$LiNO_3$+LiCl is less corrosive and its crystallization temperature is about 35 ºC lower than that of water-LiBr. The presence of lithium chloride decreases vapour pressure, lithium iodide and lithium nitrate improve solubility and lithium nitrate reduces corrosion in the system.

- Other investigations have proposed ammonia-lithium nitrate as the working pair for applications requiring high operating temperatures for the absorber and condenser of absorption chillers. Zamora et al. (2014, 2015) reported that this working pair helps to overcome some of the drawbacks of the conventional working fluids. These include crystallization and low operating pressures for water-LiBr systems and refrigerant vapour rectification at the desorber outlet for ammonia-water systems. Ammonia-lithium nitrate absorption cooling systems could also be activated by low temperature heat sources cycles, such as those found in solar cooling applications.

Table 4 summarizes the operating temperatures and the coefficient of performance of both single-effect and double-effect water-LiBr absorption chillers when they operated in each one of the five climate zones in Algeria. The OP_OFF used in the table indicates that use of the absorption chiller is not recommended in the corresponding operating conditions. This is because of crystallization of the water-LiBr solution or because of the insignificant chiller cooling capacity and coefficient of performance.

5. Conclusions

In this paper, a performance analysis of small capacity water-LiBr absorption chillers was carried out by numerical simulation at the thermal conditions of the five different Algerian climate zones. Two commercial absorption chillers were selected as case studies; a 17.6 kW Yazaki single-effect chiller and a 16 kW Broad double-effect chiller. The coefficient of performance (COP) and cooling capacity of the chillers were calculated for each climate zone at two temperatures of chilled water, namely 7 ºC and 12 ºC. Previously, a parametric study had been carried out varying the thermal conditions of the cooling medium and heat source. The results of these investigations can be summarized as follows:

- The single-effect absorption chiller was able to operate with a COP higher than 0.6 at an ambient air temperature ranging from 30 ºC to 40 ºC to produce chilled water at 7 ºC. The double-effect absorption chiller demonstrated a COP higher than 1.0 at an ambient air temperature range of 30-40 ºC to produce chilled water at 7 ºC.
- In the case of the single-effect absorption chiller, when ambient air temperature was increased from 30 ºC to 40 ºC, cooling capacity was reduced by 63% and 48% for producing chilled water at a temperature of 7 ºC and 12 ºC, respectively. The corresponding degradation rates were 56% and 44% in the case of the double-effect absorption chiller.
- In the climatic conditions in zones E1 and E2 and chilled water at 7 ºC, the single-effect absorption chiller delivered 37% of its nominal cooling capacity at heat source temperatures of 90 and 100 °C, respectively; meanwhile, the double-effect absorption chiller performed 91% of its nominal cooling capacity at heat source temperatures of 140 and 150 °C, respectively.
- In the climatic conditions of zones E3 and E4, the single-effect absorption chiller was not able to produce chilled water at 7 ºC, and the cooling capacity delivered by the double-effect absorption chiller was much lower than the nominal value even at high temperature heat sources.
- By allowing for an increase in the chilled water temperature from 7 ºC to 12°C, the single-effect absorption chiller was able to operate in the climatic conditions of zones E3 and E4 and supplied 45% and 33%, respectively, of its nominal cooling capacity with a heat source temperature of 110 °C. The double-effect absorption chiller delivered up to 80% of its nominal cooling capacity to produce chilled water at 12ºC in zones E3 and E4 applying

heat source temperatures of 155 and 160 °C, respectively.

- Regarding climate zone E5, neither the single-effect nor the double-effect absorption chiller was able to perform feasibly, either because of crystallization in the water-LiBr solution or because of very poor efficiency. This was due to the high temperatures required in the absorber and condenser. To overcome these limitations the following recommendations could be considered: (i) A geothermal heat exchanger could be used to dissipate the heat released in the absorber and condenser; (ii) The addition of other salts to lithium bromide in order to extend the solubility range of the solution, (iii) The use of an ammonia based fluid mixture such as ammonia-lithium nitrate as a working pair.
- Taking into account the cooling capacity supplied by the double-effect absorption chiller in the climatic conditions in zones E3 and E4 and the huge potential of solar irradiation available in these zones, it is much more recommendable in these hot climate zones in Algeria to use the double-effect configuration rather than the single-effect one for solar powered cooling applications.

Acknowledgements

Omar Ketfi gratefully acknowledges the Algerian Ministry of Higher Education and Scientific Research for funding his internship at the University Rovira i Virgili of Tarragona (Spain) under the National Exceptional Program PNE 2016-2017.

REFERENCES

Portail Algérien des Energies Renouvelables, Mai 2010. Le potentiel des énergies renouvelables en Algérie, le plus important d'Afrique du Nord, CDER.

Al-Alili A, Hwang Y, Radermacher R, 2014. Review of solar thermal air conditioning technologies. International journal of refrigeration. 39, 4-22.

Siddiqui M, Said S, 2015. A review of solar powered absorption systems. Renewable and Sustainable Energy Reviews. 42, 93-115.

Hidalgo M, Aumente P, Millán M, Neumann A, Mangual R, 2008. Energy and carbon emission savings in Spanish housing air-conditioning using solar driven absorption system. Applied Thermal Engineering. 28 (14-15), 1734-1744.

Mammoli A, Vorobieff P, Barsun H, Burnett R, Fisher D, 2010. Energetic, economic and environmental performance of a solar-thermal-assisted HVAC system. Energy and Buildings. 42 (9), 1524-1535.

Bermejo P, Pino F, Rosa F, 2010. Solar absorption cooling plant in Seville. Solar Energy. 84 (8), 1503-1512.

Bujedo L, Rodríguez J, Martínez P, 2011. Experimental results of different control strategies in a solar air-conditioning system at part load. Solar Energy. 85 (7), 1302-1315

Rosiek S, Batlles F, 2012. Shallow geothermal energy applied to a solar-assisted air-conditioning system in southern Spain: Two-year experience. Applied Energy. 100, 267-276.

Albers J, 2014. New absorption chiller and control strategy for the solar assisted cooling system at the German federal environment agency. International Journal of Refrigeration. 39, 48-56.

Sarabia Escriva E.J, Lamas Sivila E.V, Soto Frances V.M, 2011. Air conditioning production by a single effect absorption cooling machine directly coupled to a solar collector field, Application to Spanish climates. Solar Energy. 85 (9), 2108-2121.

Darkwa J, Fraser S, Chow D, 2012. Theoretical and practical analysis of an integrated solar hot water-powered absorption cooling system. Energy. 39 (1), 395-402.

Li M, Xu C, Hassanien R, Xu Y, Zhuang B, 2016. Experimental investigation on the performance of a solar powered lithium bromide–water absorption cooling system. International Journal of Refrigeration. 71, 46-59.

Viñas E, Best R, Lugo S, 2016. Simulation of solar air conditioning systems in coastal zones of Mexico. Applied Thermal Engineering. 97, 28-38.

Agrouaz Y, Bouhal T, Allouhi A, Kousksou T, Jamil A, Zeraouli Y, 2017. Energy and parametric analysis of solar absorption cooling systems in various Moroccan climates. Case Studies in Thermal Engineering. 9, 28-39.

CNERIB, Ministère de l'habitat, 1993. Recommandations architecturales. Editions ENAG, Alger, http://www.mhuv.gov.dz.

Borel J, 1962. Application du règlement de la construction en Algérie, définition des zones climatiques. Cahier du CSTB, N° 57, Paris.

Belgaid B, 2011. Zones climatiques de l'Algérie. Département d'architecture de Batna.

Balghouthi M, Chahbani M, Guizani A, 2012. Investigation of a solar cooling installation in Tunisia. Applied Energy. 98, 138-148.

Yazaki Corporation, www.yazakienergy.com

Xiaoyong C, Broad Co., 2004. BCT16 Commissioning Instruction and Explanation Notes, Changsha, China.

Pátek J, Klomfar J, 2006. A computationally effective formulation of the thermodynamic properties of LiBr–H_2O solutions from 273 to 500K over full composition range. International Journal of Refrigeration. 29 (4), 566-578.

Tesha, 2009. Absorption refrigeration system as an integrated condenser cooling unit in a geothermal power plant. MSc thesis, University of Iceland.

National Institute of Standards and Technology (NIST), US Department of Commerce, http://www.nist.gov/srd/nist23.cfm.

Wagner W, Pruß A, 2002. The IAPWS formulation 1995 for the thermodynamic properties of ordinary water substance for general and scientific use. J Phys Chem Ref Data. 31 (2), 387–535.

ASHRAE fundamentals, 2009. Thermodynamic properties of refrigerant. Inch-Pound Edition. Chapter 30.

Rodríguez J, 2013. Desarrollo de un Banco de Ensayos Multifuncional y de los Procedimientos para Caracterizar Equipos Térmicos de Refrigeración y Bombas de Calor de Pequeña Potencia. PhD Thesis, Rovira i Virgili University, Tarragona, Spain.

Martínez J, Martinez P, Bujedo L, 2016. Development and experimental validation of a simulation model to reproduce the performance of a 17.6 kW LiBr–water absorption chiller. Renewable Energy. 86, 473-482.

Bourouis M, Vallès M, Medrano M, Coronas A, 2005. Absorption of water vapour in the falling film of water–(LiBr+LiI+$LiNO_3$+LiCl) in a vertical tube at air-cooling thermal conditions. International Journal of Thermal Sciences. 44 (5), 491-498.

Bourouis M, Vallès M, Medrano M, Coronas A, 2005. Performance of air-cooled absorption air conditioning systems working with water- ($LiBr+LiI+LiNO_3+LiCl$). J Process Mech Eng. 219, 205-12.

Asfand F, Stiriba Y, Bourouis M, 2016. Performance evaluation of membrane-based absorbers employing $H_2O/(LiBr+LiI+LiNO_3+LiCl)$ and $H_2O/(LiNO_3+KNO_3+NaNO_3)$ as working pairs in absorption cooling systems. Energy. 115, 781-790.

Zamora M, Bourouis M, Coronas A, Vallès M, 2014. Pre-industrial development and experimental characterization of new air-cooled and water-cooled ammonia/lithium nitrate absorption chillers. International Journal of Refrigeration. 45, 189-197.

Zamora M, Bourouis M, Coronas A, Vallès M, 2015. Part-load characteristics of a new ammonia/lithium nitrate absorption chiller. International Journal of Refrigeration. 56, 43-52.

Ketfi O, Merzouk M, Kasbadji Merzouk N, Metennani S.E, 2015. Performance of a Single Effect Solar Absorption Cooling System (Libr-H_2O). Energy Procedia. 74, 130-138.

Seltzer P, 1949. Le climat de l'Algérie. Alger.

Djenas S, 1984. Elaboration des Zones Climatiques en Algérie. PFE, CSTB.

Keith F.H, Radermacher R, Klein S. A, 2016. Absorption Chiller and Heat Pumps. Second Edition, CRC, USA.

McQuiston F.C, Parker J.D, Spitler J.D, 2005. Heating, Ventilating and Air Conditioning: Analysis and Design. Sixth Edition, Wiley, USA.

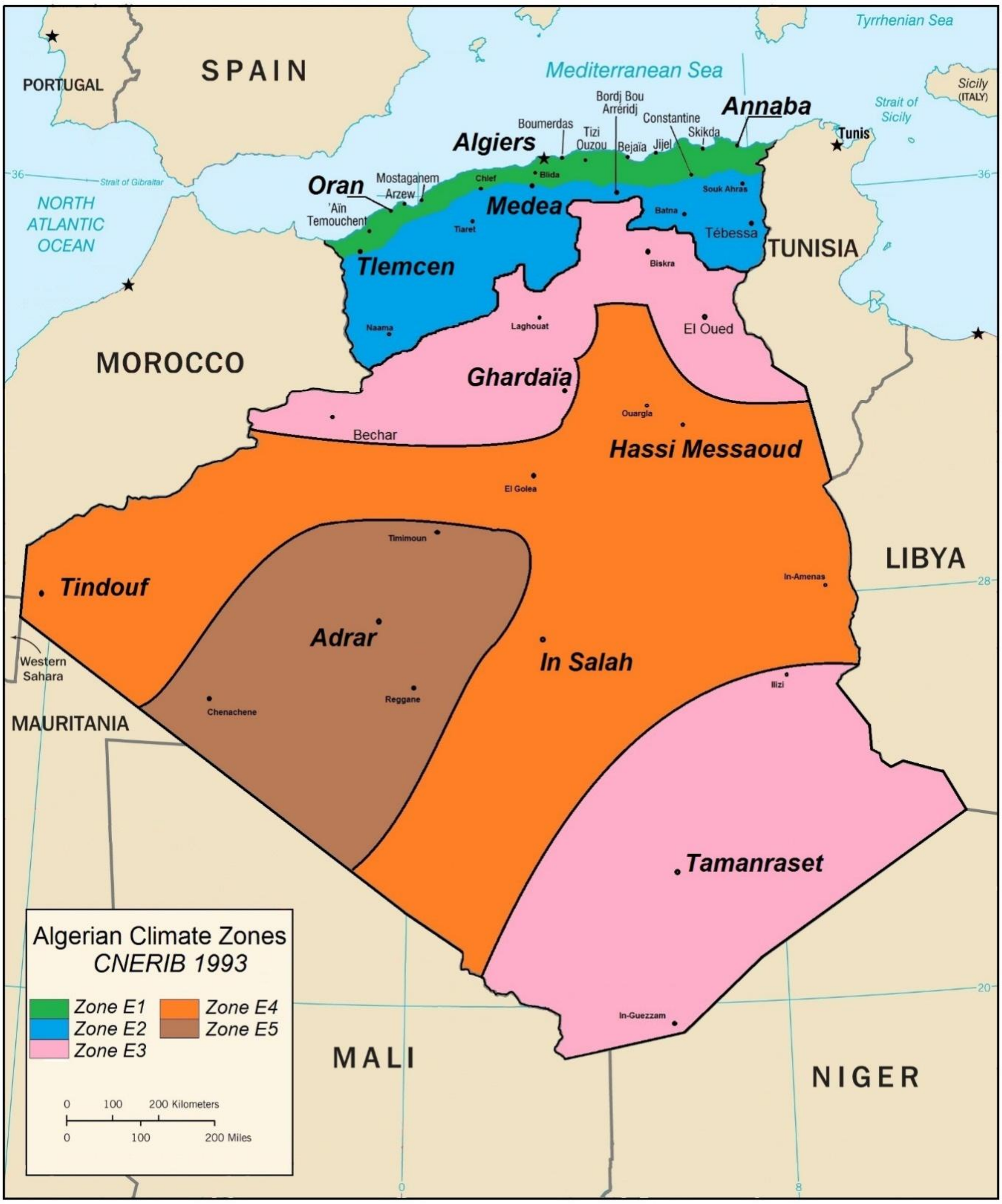

Figure 1. Climate zones in Algeria (CNERIB 1993).

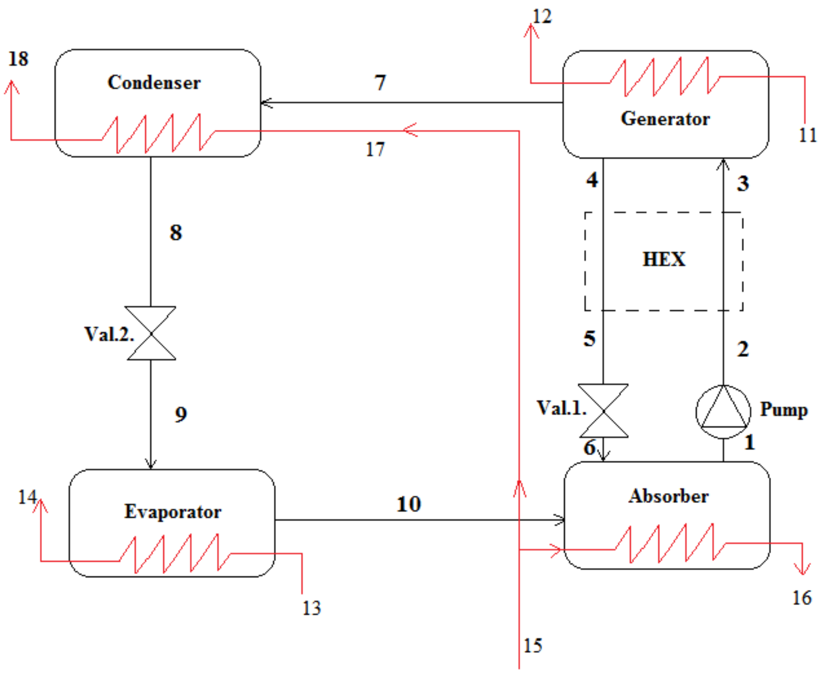

Figure 2. Schematic flow diagram of the Yazaki single-effect water-LiBr absorption chiller.

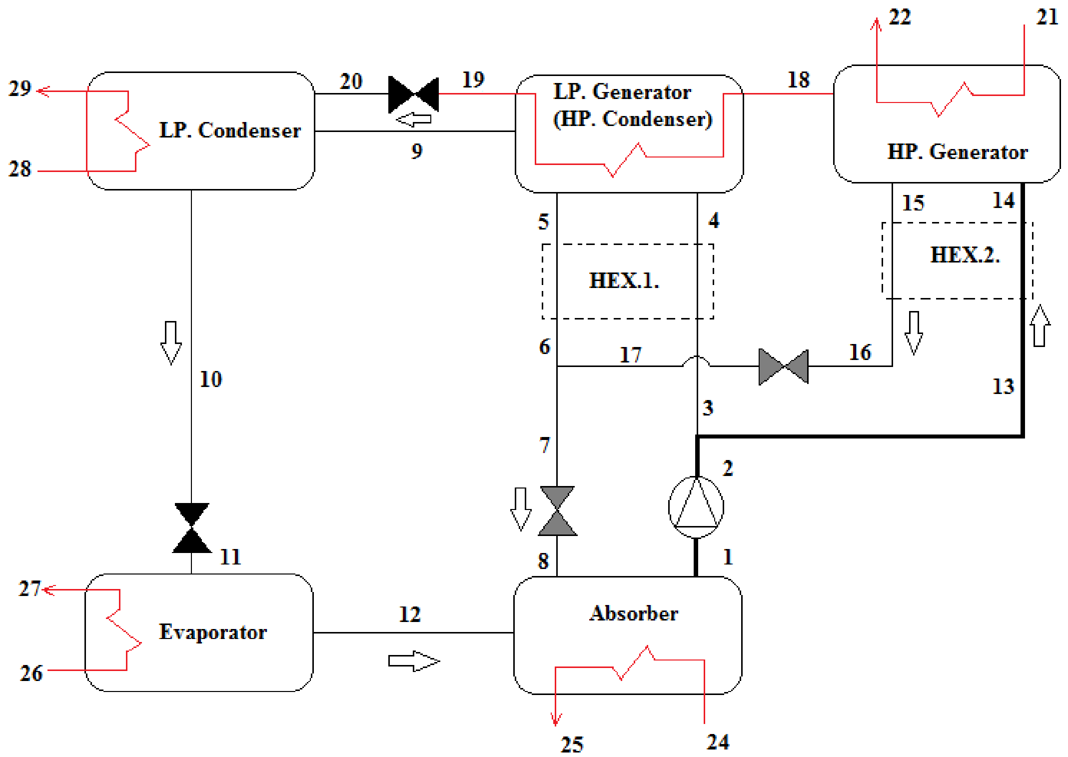

Figure.3. Schematic flow diagram of the Broad double-effect water-LiBr absorption chiller.

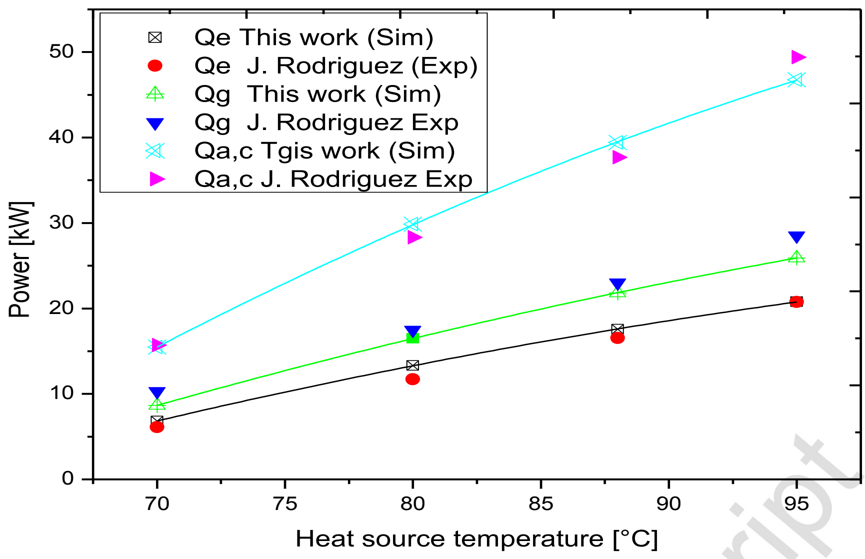

Figure 4. Model validation with experimental data from the Yazaki absorption chiller.

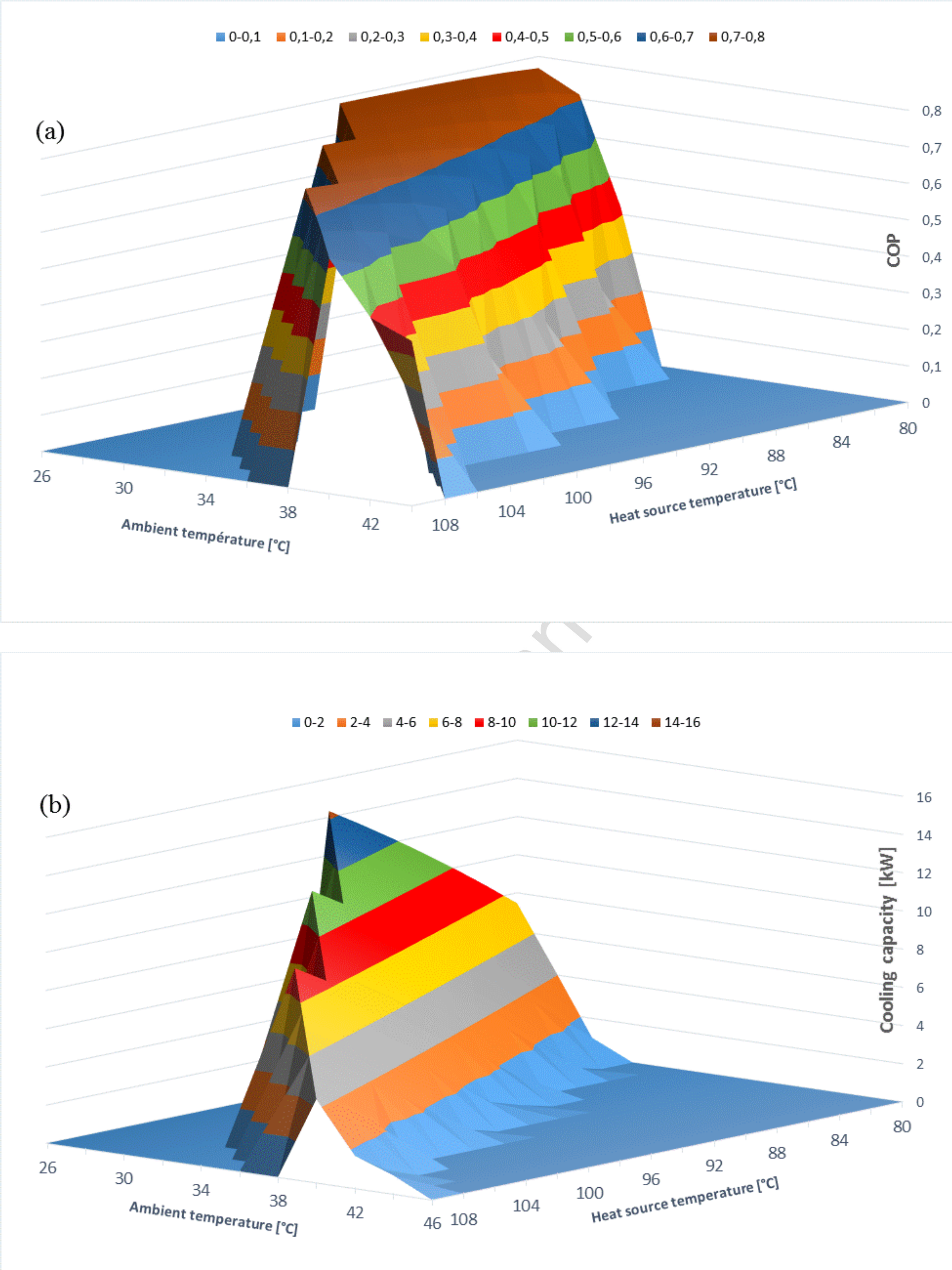

Figure 5. Variation of the coefficient of performance and cooling capacity of the single-effect absorption cycle versus ambient air and heat source temperatures for a chilled water temperature of 7 °C.

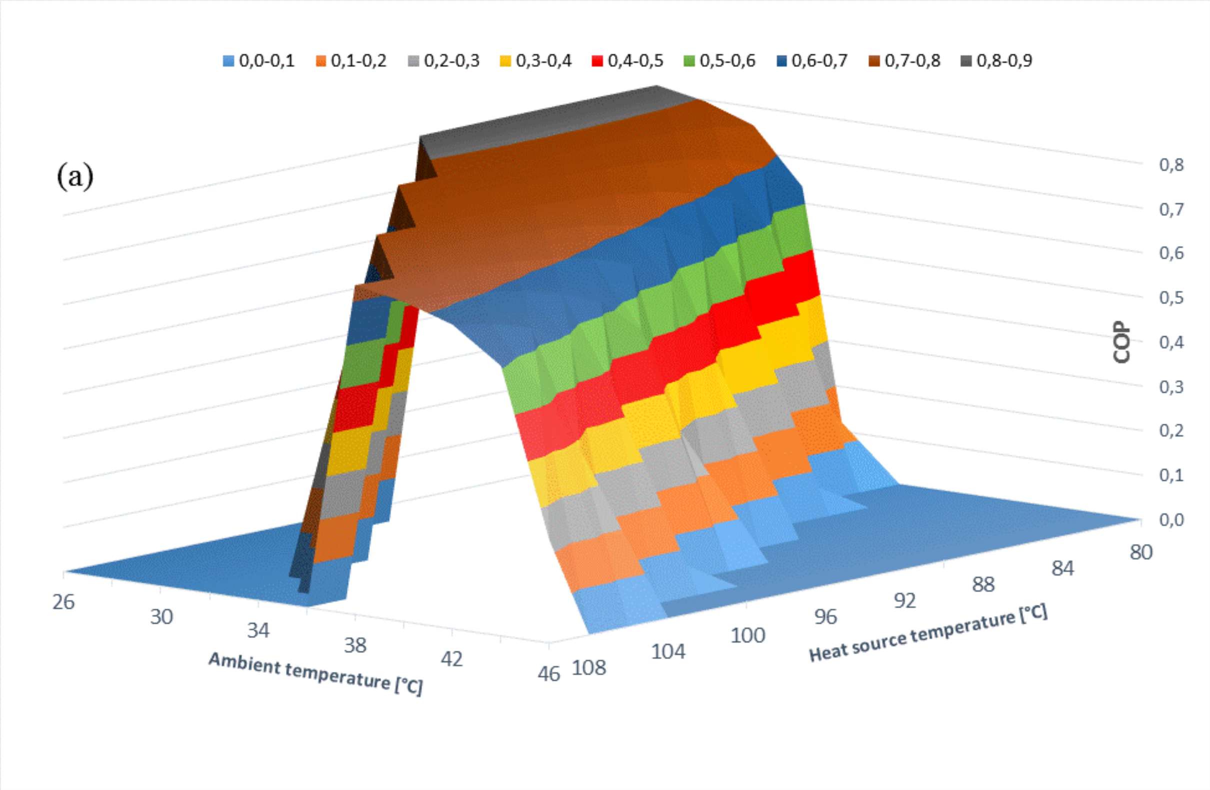

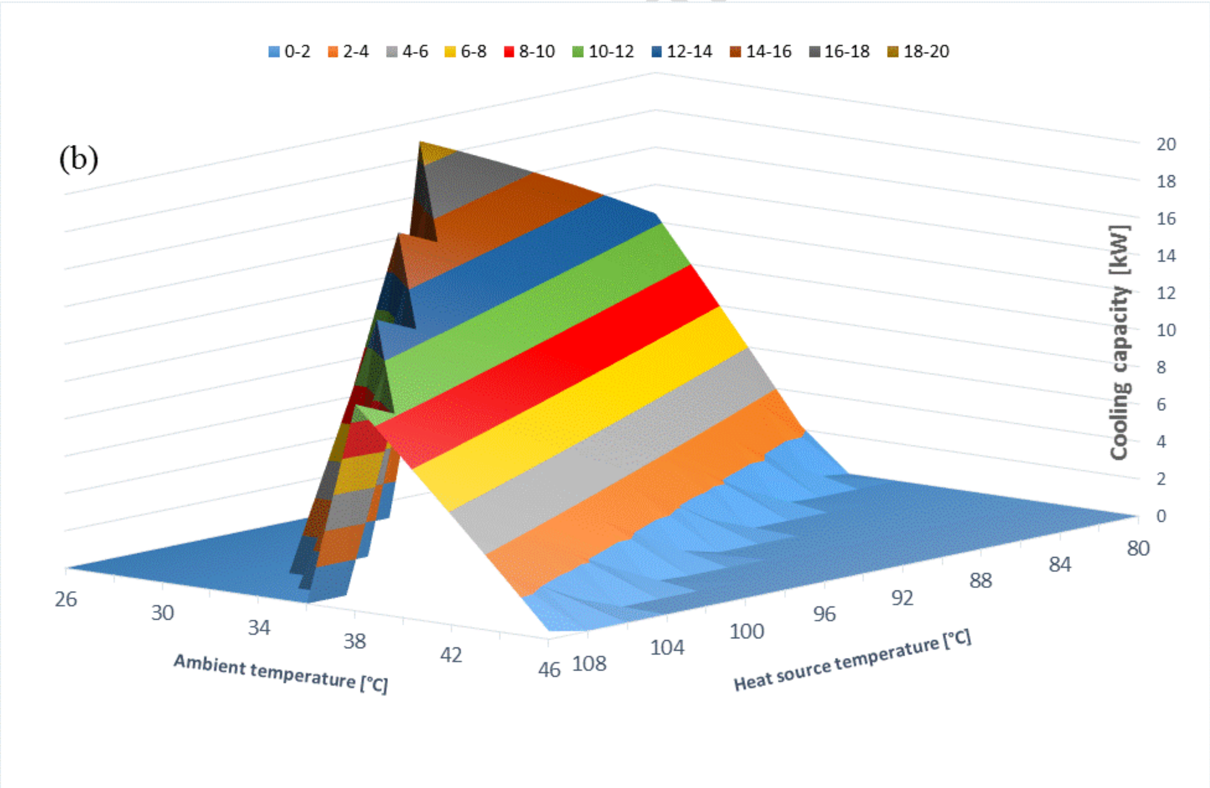

Figure 6. Variation of the coefficient of performance and cooling capacity of the single-effect absorption chiller versus ambient air and heat source temperatures for a chilled water temperature of 12 ºC.

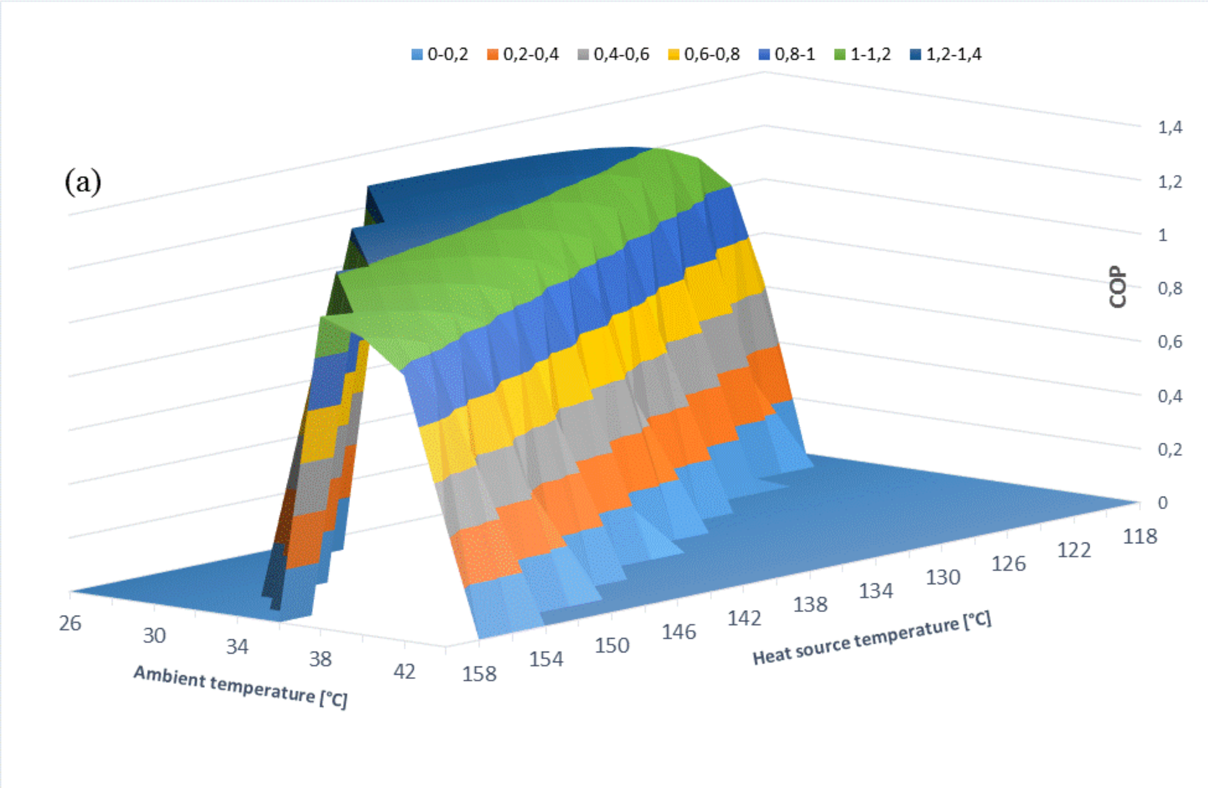

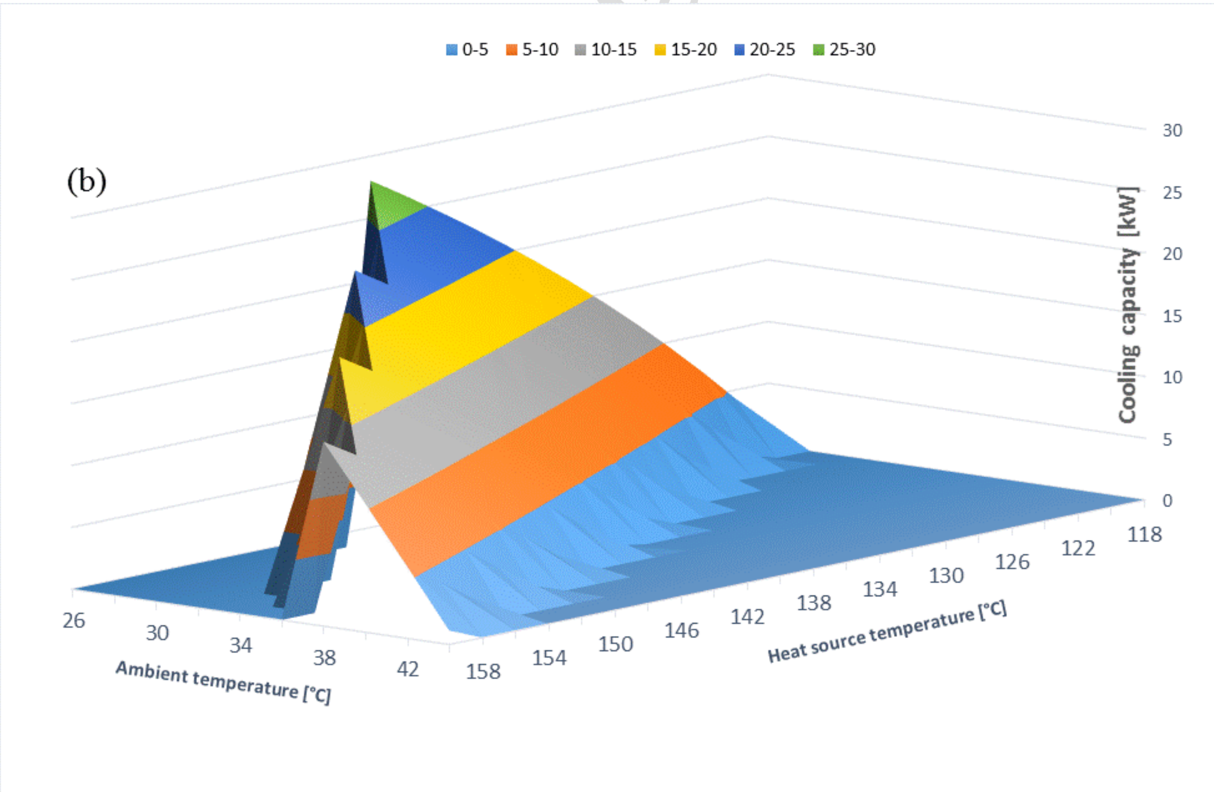

Figure 7. Variation of the coefficient of performance and cooling capacity of the double-effect absorption chiller versus ambient air and heat source temperatures for a chilled water temperature of 7 ºC.

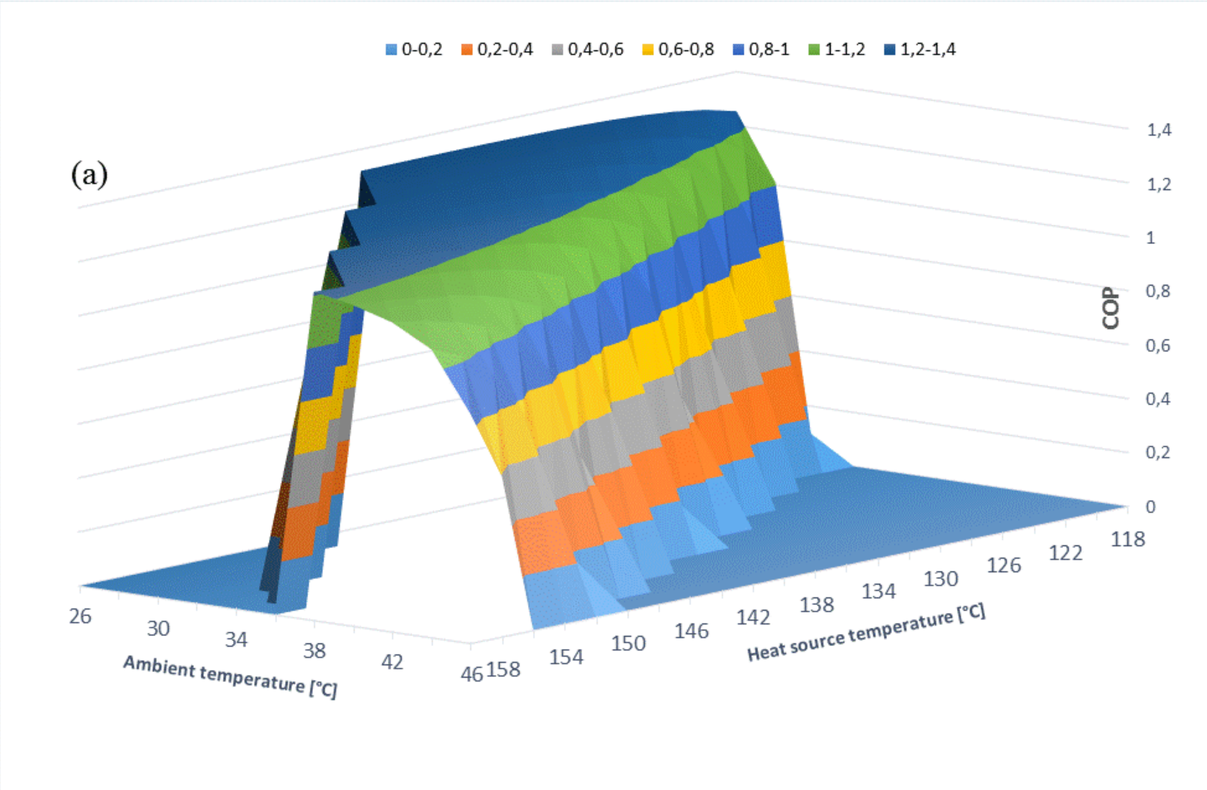

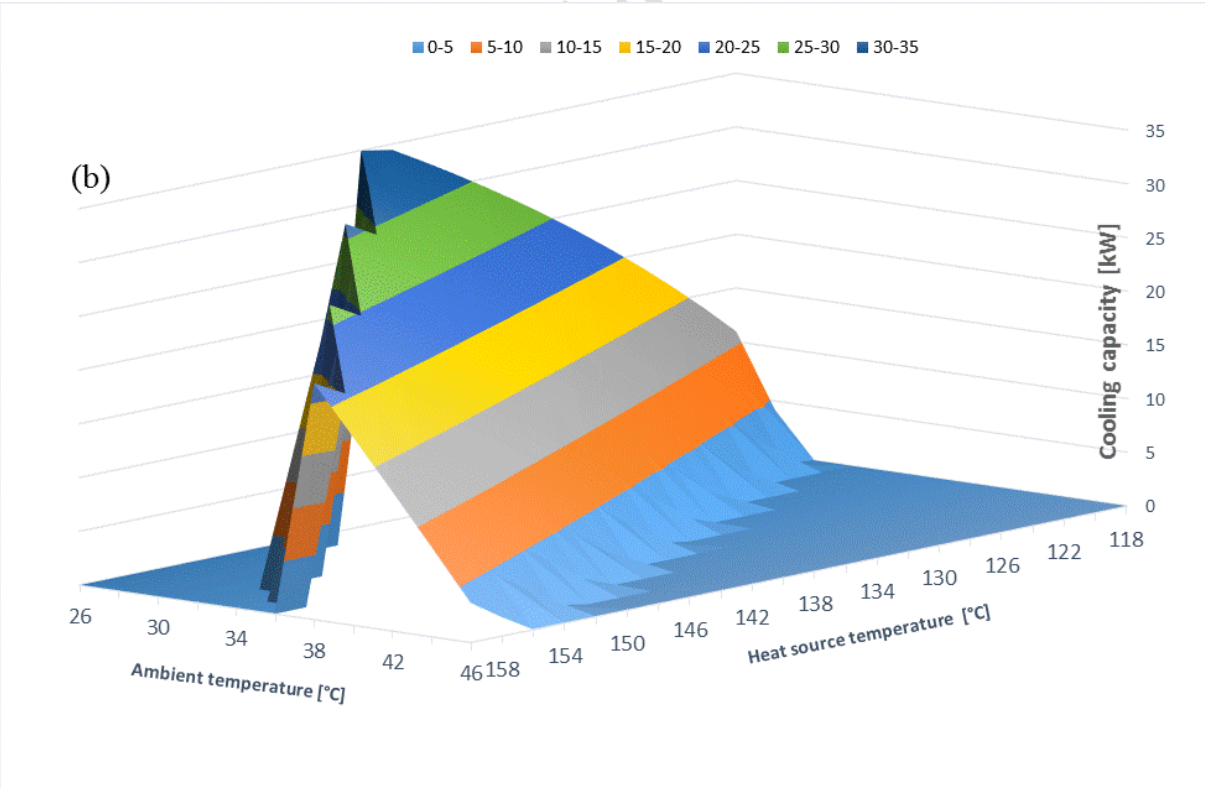

Figure 8. Variation of the coefficient of performance and cooling capacity of the double-effect absorption chiller versus ambient air and heat source temperatures for a chilled water temperature of 12 ºC.

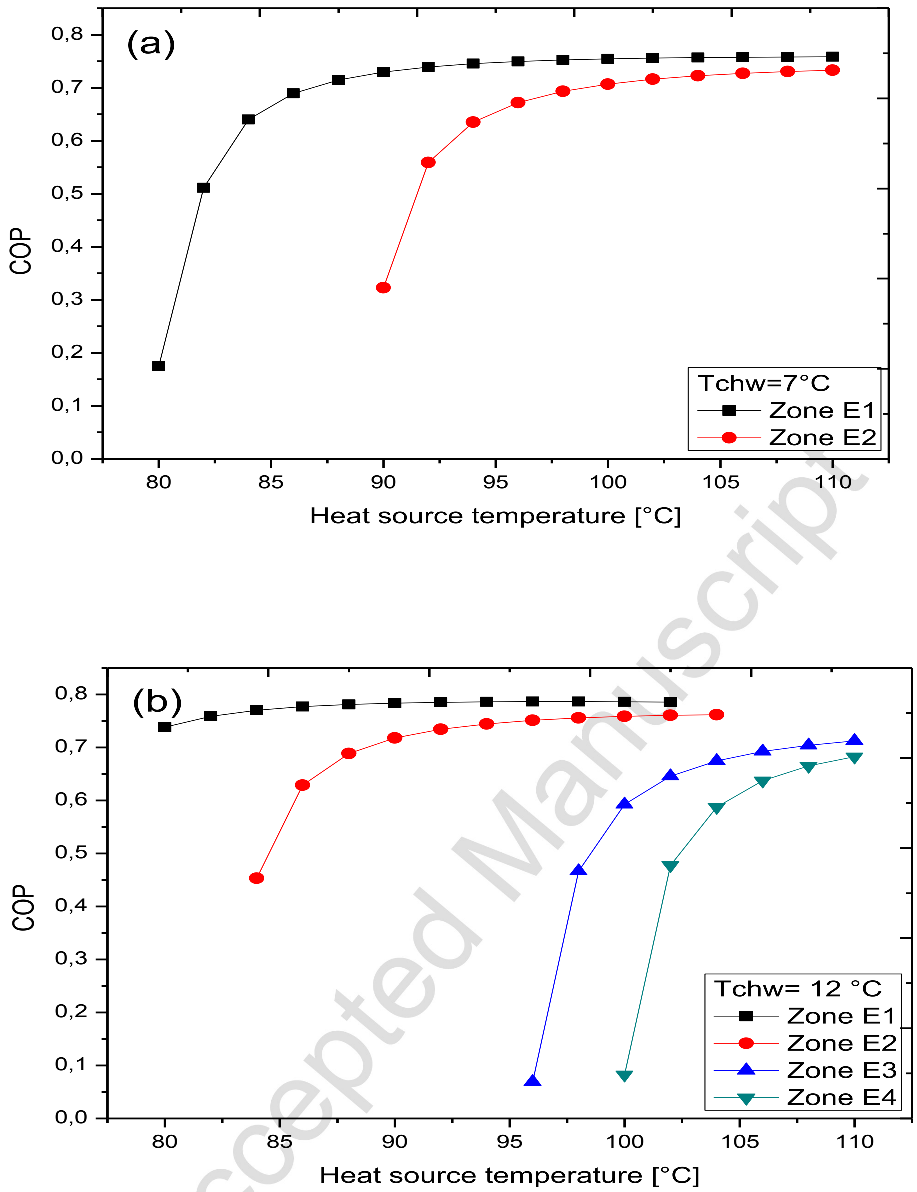

Figure 9. COP versus heat source inlet temperature for the single-effect absorption chiller at chilled water temperatures of 7 and 12 ºC.

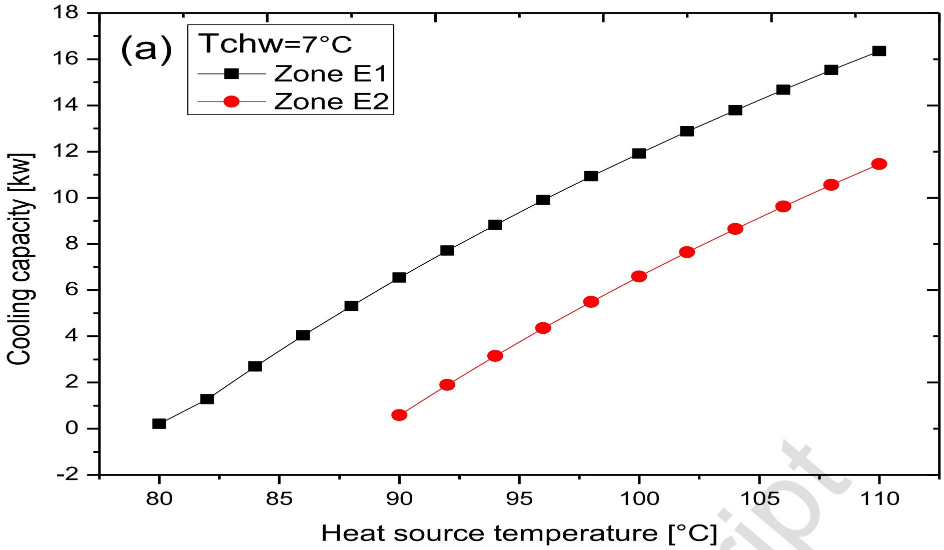

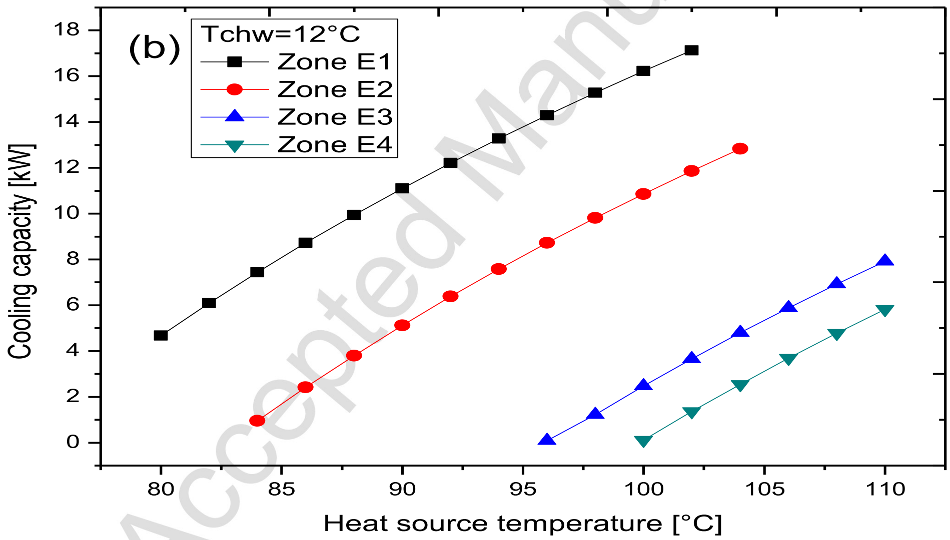

Figure 10. Cooling capacity versus heat source inlet temperature for the single-effect absorption chiller at chilled water temperatures of 7 and 12 ºC.

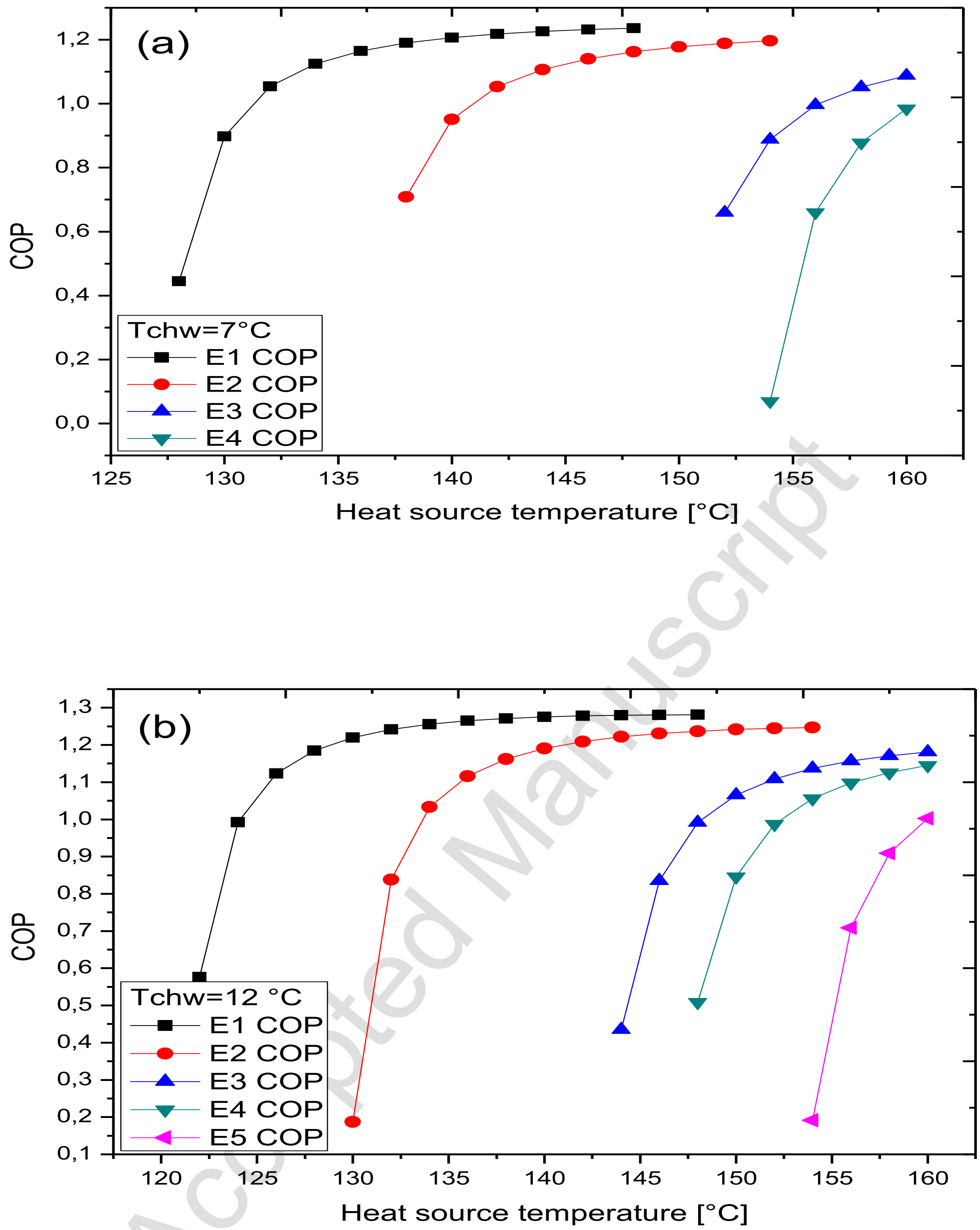

Figure 11. COP versus heat source inlet temperature for the double-effect absorption chiller at chilled water temperatures of 7 and 12 ºC.

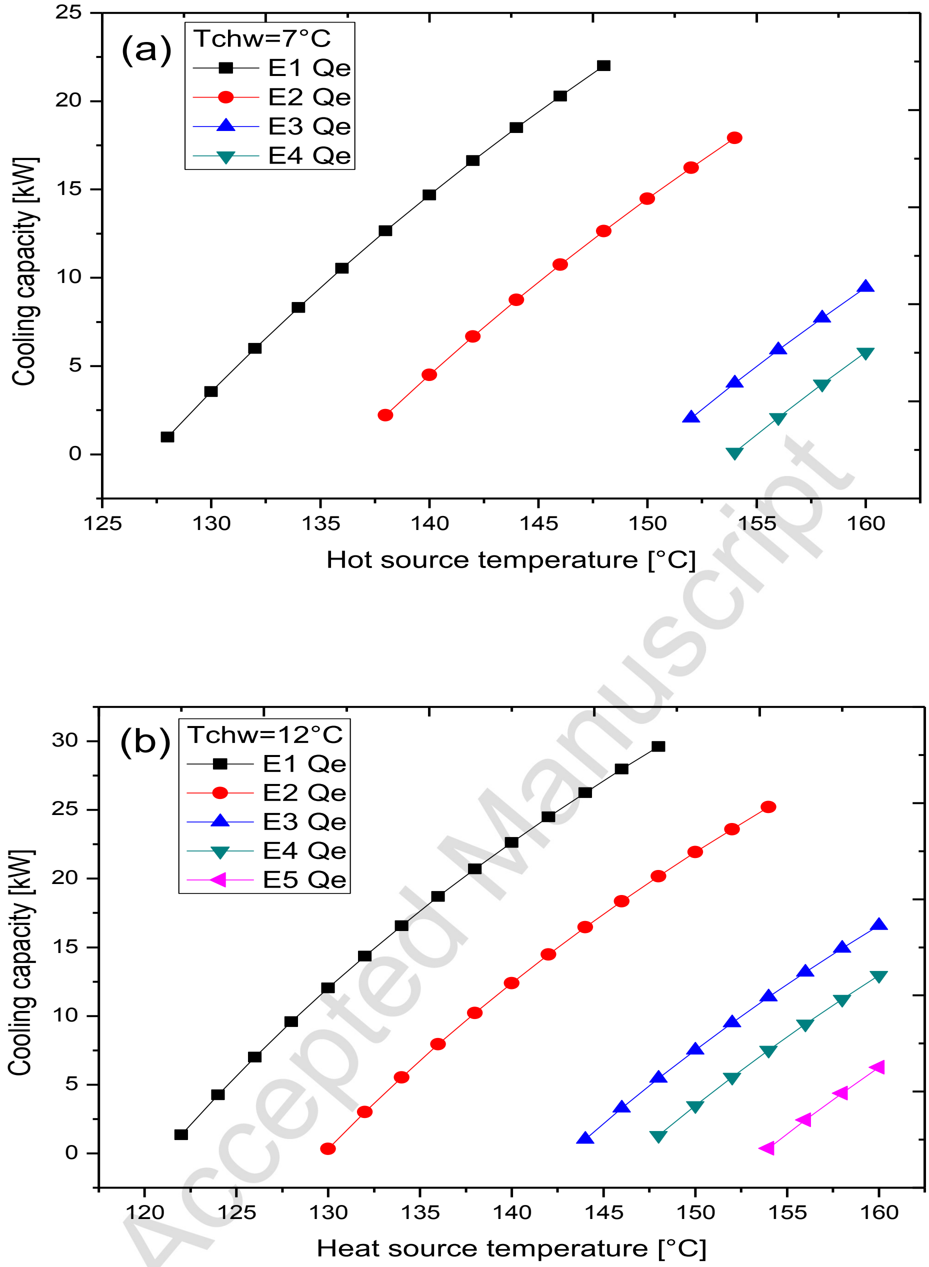

Figure 12. Cooling capacity versus heat source inlet temperature for the double-effect absorption chiller at chilled water temperatures of 7 and 12 ºC.

Table 1. Data on the five climate zones in Algeria (ONM data 1974-1984; Belgaid (2011)).

Climate zone	July: Hottest month of the year Temperature [°C]			Global irradiation on horizontal surface [Wh m^{-2}]
	mean	min	max	
E1: Coastal zone	24.2	18.4	30.6	6936
E2: Mountains and highlands	24.9	14.7	34.5	7494
E3: Pre-Sahara	32.5	24.5	40.4	6924
E4: Sahara	33.4	24.3	42.0	7516

E5: Sahara	36.5	26.8	44.9	8108

Table 2. Constants used in Eq. (4).

LiBr mass concentration (%)	A	B	C
$x < 48.5$	−0.253	25.107	−398.3
$48.5 < x < 57.2$	−0.3080928653	38.51957477	−919.4
$57.2 < x < 65.5$	−0.308288545	42.7386184	−1159.4
$x \geq 65.5$	−0.3391180069	58.34181996	−2046.536869

Table 3. Input parameters used in the simulation of the Yazaki single-effect and Broad double-effect water-LiBr absorption chillers.

Parameter	Value
Yazaki WFC-SC5	
Nominal conditions	
Cooling capacity	17.6 kW
Chilled water temperature inlet/outlet	12/7 °C
Hot water temperature inlet/outlet	88/83 °C
Cooling water temperature inlet/outlet	31/35 °C
Mass flowrate of the solution leaving the absorber	$4\ 10^{-2}$ kg s^{-1}
Efficiency of the solution heat exchanger	0.64
Coefficient of performance (COP)	0.7
Parametric study	
Outlet chilled water temperature	7 to 12 °C
Inlet hot water temperature	80 to 110 °C
Ambient air temperature	26 to 46 °C
Broad BCT 16	
Nominal conditions	
Cooling capacity	16 kW
Chilled water temperature inlet/outlet	14/7 °C
Heat source	Steam
Cooling water temperature inlet/outlet	32/38
Mass flowrate of the solution leaving the absorber	$7\ 10^{-2}$ kg s^{-1}
Efficiency of the solution heat exchangers	0.60
Coefficient of performance (COP)	1.0
Parametric study	
Outlet chilled water temperature	7 to 12 °C
Heat source temperature	118 to 160 °C
Ambient air temperature	26 to 46 °C
Temperature gradients between the internal streams and external circuits for both absorption chillers	
Generator & Evaporator	3 ºC
Absorber & Condenser (Indirect cooling)	7.5 ºC

Table 4. Thermal conditions and performance of the single-effect and double-effect water-LiBr absorption chillers which operated in the five climate zones in Algeria.

Climate Zone	Maximum ambient air temperature [°C]	Chilled water temperature [°C]	Single-effect chiller		Double-effect chiller		Recommendations
			Heat source temperature [°C]	COP	Heat source temperature [°C]	COP	
E1	30.6	7 12	98-110 88-100	0.75 0.78	146-148 146-148	1.23 1.28	
E2	34.5	7 12	110 104	0.73 0.76	154 150-154	1.19 1.24	
E3	40.4	7 12	OP_OFF* 110	OP_OFF* 0.71	OP_OFF* 160	OP_OFF* 1.18	
E4	42.0	7 12	OP_OFF* 110	OP_OFF* 0.68	OP_OFF* 160	OP_OFF* 1.14	
E5	44.9	7 12	OP_OFF* OP_OFF*	OP_OFF* OP_OFF*	OP_OFF* OP-OFF*	OP_OFF* OP_OFF*	• Geothermal cooling of the absorber and condenser. • Use of water/multi-salts working pairs such a water-LiBr+LiI+$LiNO_3$+LiCl. • Use of ammonia based working pairs such as NH_3-$LiNO_3$.

**OP_OFF: Use of the absorption chiller is not recommended in the corresponding operating conditions*